2016 Spring Technical Meeting
Eastern States Section of the Combustion Institute
Hosted by Princeton University
March 13-16, 2016

Gas-Phase Interactions of Phosphorus Containing Compounds with Cup-Burner Diffusion Flames

Fumiaki Takahashi[1], *Viswanath R. Katta*[2], *Gregory T. Linteris*[3], *Valeri I. Babushok*[3]

[1]*Department of Mechanical and Aerospace Engineering, Case Western Reserve University, Cleveland, Ohio*
[2]*Innovative Scientific Solutions, Inc., Dayton, Ohio*
[3]*National Institute of Standards and Technology, Gaithersburg, Maryland*

The effects of phosphorus-containing compounds (PCC) on the extinguishment and structure of methane-air co-flow diffusion flames, in the cup-burner configuration, have been studied computationally. Dimethyl methylphosphonate (DMMP), trimethyl phosphate (TMP), or phosphoric acid was added to either the air or fuel flow. Time-dependent axisymmetric computation was performed with full gas-phase chemistry and transport to reveal the flame structure and inhibition process. A detailed chemical-kinetics model (77 species and 886 reactions) was constructed by combining the methane-oxygen combustion and phosphorus inhibition chemistry. A simple model for radiation from CH_4, CO, CO_2, and H_2O based on the optically thin-media assumption was incorporated into the energy equation. The two-zone flame structure was formed for DMMP and, to a lesser extent, TMP, due to the heat release by the inhibitor itself. The inhibitor effectiveness was calculated as the minimum extinguishing concentrations (MECs) of CO_2 (added to the oxidizer) as a function of the PCC loading (added to the oxidizer or fuel stream). The calculated MEC of CO_2 without an inhibitor was in good agreement with the measured value. For moderate DMMP loading to the air (<1 %), the measured value became significantly smaller, presumably due to particle formation in the experiment. An inhibitor in the oxidizer flow was an-order-of-magnitude more effective compared to that in the fuel flow in gas-phase inhibition of co-flow diffusion flames.

1. Introduction

Phosphorus-containing compounds (PCCs) are known to be effective at reducing flammability of polymers, with some ambiguity as to whether their effectiveness is due to gas phase reactions involving phosphorus intermediates, or a condensed-phase action [1]. The use of PCCs as fire retardant (FR) additives to plastics has increased dramatically in recent years [2-6]. In this application, the relative importance of gas phase chemistry and solid-phase effects such as char promotion has been debated, with recent work suggesting comparable importance for the two mechanisms, depending on the specific PCC chemistry [3, 7-9]. Due to environmental and health concerns on the most common gas-phase active FR formulations, bromine-containing compounds with antimony trioxide, PCCs are considered as the chemical systems of highest interest to polymer companies and fire retardant manufactures, and the subject of the most

intense recent investigations [10, 11]. While FRs added to polymers increase their ignition time and reduce their heat release rates when burning [1, 4, 12], PCCs have also been evaluated as potential halon replacements for fire suppression [13] using cup burner, streaming tests [14, 15] and opposed-jet diffusion flames [16]. Further understanding of how PCCs affect flames is important for their efficient use.

A model for the gas-phase chemical kinetics of phosphorus compounds has been developed over the years. The decomposition of PCCs is a relatively fast, complicated process in a flame reaction zone. Once it has decomposed, PCC's main products (PO_2, PO, HOPO and $HOPO_2$) participate in catalytic radical recombination cycles that inhibit the flame. Simplified versions of the main cycles are shown in Figure 1. Sensitivity and reaction pathway analyses show two main inhibition cycles involving reactions of PO_2, HOPO and $HOPO_2$ species ($PO_2 \Leftrightarrow$ HOPO and $PO_2 \Leftrightarrow HOPO_2$):

(1) $H + PO_2 + M \rightarrow HOPO + M$
$OH + HOPO \rightarrow H_2O + PO_2$
$H + HOPO \rightarrow H_2 + PO_2$
$O + HOPO \rightarrow OH + PO_2$

(2) $OH + PO_2 + M \rightarrow HOPO_2 + M$
$H + HOPO_2 \rightarrow H_2O + PO_2$

Each step of these cycling sequences involves scavenging of H, O, and OH radicals, decreasing their concentration, and correspondingly, the flame reaction rate.

The effects of dimethylmethylphosphonate (DMMP, $PO[CH_3][OCH_3]_2$) in methane-air co-flow diffusion flames, in the cup-burner configuration, have recently been investigated experimentally [17] at the National Institute of Standards and Technology (NIST). By using comprehensive numerical simulations, the present authors have studied the flame structure [18] and inhibition (or combustion enhancement) [19-21] processes in the cup-burner flames. This paper reports the numerical results for three PCCs: DMMP, tetramethylphosphate ($PO[OCH_3]_3$), and phosphoric acid ($PO[OH]_3$). As DMMP and TMP have a significant heating value (due to methyl groups attached to the phosphorus atom), phosphoric acid is also used for a comparison (since it provides the chemical inhibition without the fuel effect). The additive affects the flame structure, which then changes the additive effectiveness. The overall goal of the present work is to understand how the properties of flames interact with the gas-phase inhibition. The knowledge of detailed flame structure that affects fire retardant effectiveness will help to understand the reasons for the variation of effectiveness for phosphorus with flame type.

2. Computational Methods

A time-dependent, axisymmetric numerical code (UNICORN) [22, 23] is used for the simulation of diffusion flames stabilized on the cup burner. A clustered mesh system is employed to trace the gradients in flow variables near the flame surface. The thermo-physical properties such as enthalpy, viscosity, thermal conductivity, and binary molecular diffusion of all of the species are calculated from the polynomial curve fits developed for the temperature range 300 K to 5000 K. Mixture viscosity and thermal conductivity are estimated using the Wilke and Kee expressions, respectively. A simple radiation model based on the optically thin-media assumption for CH_4, CO, CO_2, H_2O and soot is considered. A comprehensive reaction mechanism (77 species and 886 elementary reactions) is assembled from a detailed reaction mechanism of GRI-V3.0 [24] for methane-oxygen combustion and a phosphorus mechanism [25].

The finite-difference forms of the momentum equations are obtained using an implicit QUICKEST scheme [22], and those of the species and energy equations are obtained using a hybrid scheme of upwind and central differencing. A physical domain of 200 mm by 47.5 mm is used with a 351 × 151 non-uniform grid system that yields 0.2 mm by 0.15 mm minimum grid spacing in the *z* and *r* directions, respectively, in the flame zone. The outflow boundary in *z* direction is located sufficiently far from the burner exit ≈14 fuel-cup radii) such that propagation of boundary-induced disturbances into the region of interest is minimal. The cup burner outer diameter is 28 mm and the chimney inner diameter is 95 mm. The burner wall (1-mm long and 1-mm thick tube) temperature is set at 600 K, and the wall surface is under the no-slip velocity condition. The mean gas velocities are set at 1.24 cm/s and 15.5 cm/s, respectively, for the fuel (methane) and oxidizer streams and a temperature of 374 K. The air velocity is in the middle of the so-called "plateau region" [19], where the extinguishing agent concentration is independent of the oxidizer velocity.

Validation of the UNICORN code has been performed for a variety of flame systems, fuels, and inhibitors with the kinetic model used. The predicted global strain rates at extinction of methane-air opposing-jet flames at the reactant temperature of 373 K are 380 s^{-1} without the inhibitor, which is close to the measured value (360 s^{-1}) [16], and those with DMMP added to the flames with different stretch rates are within a range of 10 % of the experiments.

3. Results and Discussion

First, stable flames with an inhibitor were calculated by increasing incrementally (starting at 0) the loading of the inhibitor in the oxidizer or fuel stream. Then, the flame extinguishing conditions were determined by increasing the CO_2 volume fraction (X_{CO2}) in the oxidizer (starting at 0; in increments of < 1 % of X_{CO2} as the limit approached) until the flame blew off. The process was repeated at different inhibitor loadings. Figure 1 shows the calculated and measured [17] inhibitor effectiveness expressed as the MECs of CO_2 added to the oxidizer as a function of the inhibitor loading: (a) added to the oxidizer or (b) fuel stream. The calculated MEC without DMMP was X_{CO2} = 0.199, which was in reasonable agreement (≈ 7 %) with measurement (0.185 at 373 K) [17]. With an addition of DMMP to the oxidizer (Fig. 1a) at very low volume fractions ($X_{DMMP\text{-}O}$ <0.003), both measured and calculated MECs of CO_2 decreased rapidly as a result of efficient chemical inhibition. The calculated MEC of CO_2 became significantly larger than the measured value, probably because of particle formation just outside the actual flames with DMMP [17]. Since the calculation did not take into account particle formation, the actual flame temperature could be much lower than the calculation due to the radiative heat loss from the high-temperature particles, formed on the air side of the flame zone [17], thus requiring much lower X_{CO2} at extinguishment. As the DMMP volume fraction was increased further, the rate of decrease (slope) of the MEC curves decreased, particularly for the experiment, and thus the two curves crossed at $X_{DMMP\text{-}O}$ = 0.012.

In the experiment [17], the marginal effectiveness of the DMMP diminished, and for $X_{DMMP\text{-}O}$ > 0.07, the additional DMMP was essentially ineffective. The behavior for DMMP was very similar to that observed for metallic compounds added to cup-burner flames [18]. The loss of effectiveness for the metals was believed to be due to particle formation (which acted as a sink for the active gas-phase intermediate species that catalytically recombined radicals). Premixed

flame structure calculations [17] implied that DMMP addition reduced the concentrations of the chain-carrier radicals (H, O, and OH) to the equilibrium levels so that additional DMMP had little effect on the flame.

The MEC curve for TMP followed closely that for DMMP as the concentrations profiles of the main decomposition products (PO_2, HOPO and $HOPO_2$) were nearly the same. On the other hand, the inhibition effectiveness of phosphoric acid was higher than those of DMMP and TMP. Unlike DMMP and TMP, which have a significant heating value due to methyl groups attached to the phosphorus atom, phosphoric acid provides the chemical inhibition without the fuel effect.

The inhibitor effectiveness of PCCs was reduced markedly when added to the fuel stream (Fig. 1b). As the DMMP volume fraction was increased, the measured MEC of CO_2 decreased rapidly and became nearly ineffective for $X_{DMMP\text{-}F} > 0.01$. The calculated MEC of CO_2 for DMMP decreased linearly, showing no synergistic effect with CO_2. The volume fraction of DMMP required to extinguish without CO_2 ($X_{DMMP\text{-}F} = 0.281$) was an order of magnitude larger than that for the addition to the oxidizer ($X_{DMMP\text{-}O} = 0.0181$).

Figure 2 shows the calculated structure of methane cup-burner flames near extinguishment. The flame with DMMP added to the oxidizer (Fig. 2a) shows the two-zone flame structure [21] due to the heat release by the inhibitor itself on the air side of the main flame zone. There is no outer heat-release zone for DMMP added to the fuel (Fig. 2b). The flame with TMP added to the oxidizer (Fig. 2c) also shows, to a lesser extent, the two-zone flame structure. By contrast, the flame with phosphoric acid added to the oxidizer (Fig. 2d) shows the main flame zone only with relatively high flame temperature. The maximum flame temperature was substantially higher (> 2100 K) for DMMP or TMP added to the oxidizer. The radial distributions of the species volume fractions across the flame base (not shown) revealed that the maximum H-atom concentration decreased to constant values ($X_H \approx 0.0002$ for the PCC loading to the oxidizer, $X_H \approx 0.00024$ for the PCC loading to the fuel).

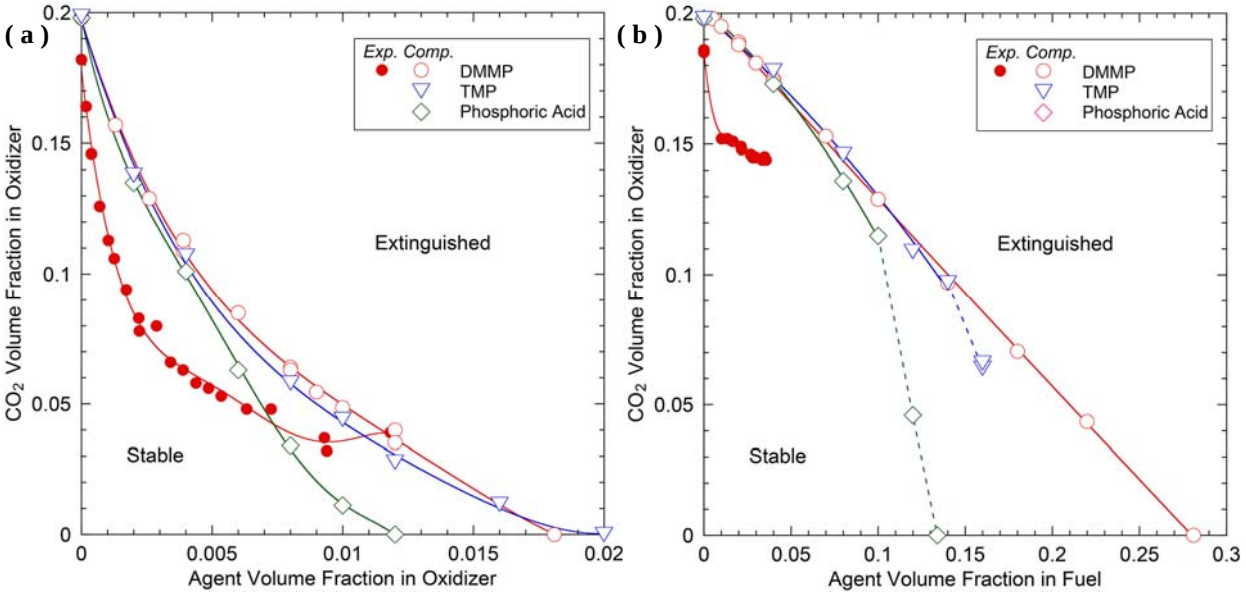

Figure 1 Minimum extinguishing concentrations of CO_2 in methane cup-burner flames: (a) both CO_2 and DMMP added to the oxidizer and (b) CO_2 added to the oxidizer and DMMP to the fuel flow.

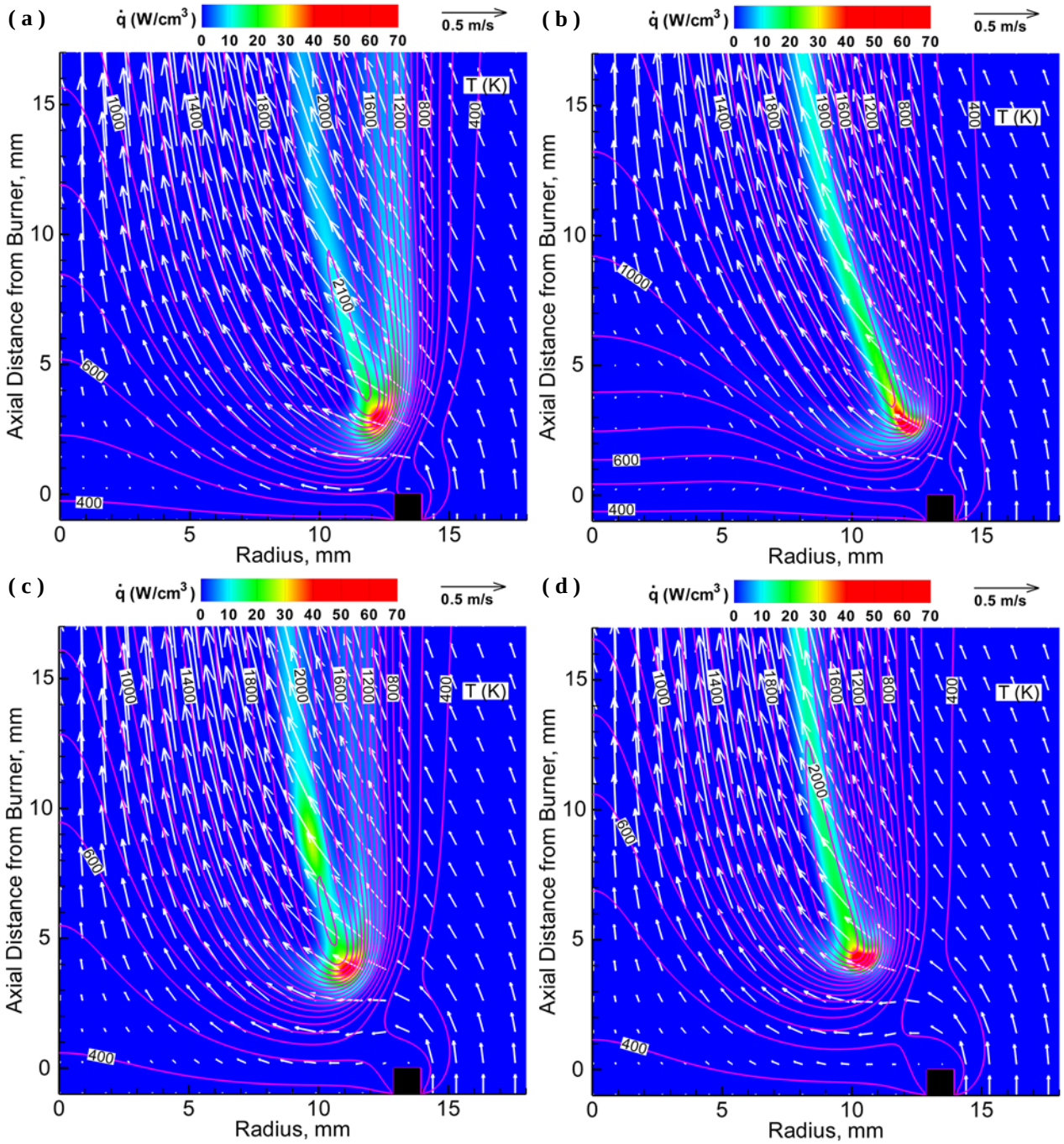

Figure 2: Calculated structure of methane cup-burner flames with agents: (a) DMMP added to the oxidizer at $X_{DMMP\text{-}O}$ = 0.018, (b) DMMP added to the fuel at $X_{DMMP\text{-}F}$ = 0.28, (c) TMP added to the oxidizer at $X_{TMP\text{-}O}$ = 0.016, and (d) phosphoric acid added to the oxidizer at $X_{PA\text{-}O}$ = 0.011.

Conclusions

The physical and chemical effects of the PCCs, acting in the gas phase, on the structure and inhibition of methane-air co-flow diffusion flames, in the cup-burner configuration, were studied computationally. The inhibitor effectiveness was calculated as the MECs of CO_2 (added to the oxidizer) as a function of the PCC loading (added to the oxidizer or fuel stream). The

effectiveness of PCCs added to the oxidizer was high. The two-zone flame structure was predicted with the DMMP (or TMP) addition to the oxidizer due to the reactions of the inhibitor itself. PCCs in the fuel stream were an-order-of-magnitude less effective in gas-phase inhibition of co-flow diffusion flames. This result is a drawback for fire retardants added to solid materials, while it is beneficial to fire suppressants deployed into the surrounding air. The inhibition processes in co-flow diffusion flames are influenced strongly by transport phenomena as well as chemical kinetics because of (1) a small stoichiometric mixture fraction (0.055 for methane), (2) which results in the flame location on the oxidizer side of the dividing streamline, and (3) thus, for the inhibitor added to the fuel, reducing the concentrations of active phosphorus intermediate species (PO_2, HOPO, and $HOPO_2$) in the flame stabilizing region so that the catalytic reactions to recombine the chain-carrier radicals (H, O, and OH) were relatively slow.

Acknowledgements

This work was supported under a Cooperative Agreement between the National Institute of Standards and Technology and FXT Consulting, LLC.

References

[1] G.T. Linteris, Gas-phase Mechanisms of Fire Retardants, NIST IR 6889, NIST, Gaithersburg, MD, 2002.
[2] H. Staendeke D.J. Scharf, Kunststoffe-German Plastics 79 (1989) 1200-1204.
[3] G. Avondo, C. Vovelle, R. Delbourgo, Combust. Flame 31 (1978) 7-16.
[4] S.V. Levchik, Introduction to Flame Retardancy and Polymer Flammability, In: Flame Retardant Polymer Nanocomposites (A.B. Morgan and C.A. Wilkie, eds.), John Wiley & Sons, Inc., 2007, pp.1-29.
[5] L.M. Sherman, Plastics Technol. 38 (1992) 102-105.
[6] S. Shelly, Chem. Eng. 100 (1993) 71-73.
[7] S.K. Brauman, Journal of Fire Retardant Chem. 4 (1977) 18-37.
[8] J. Green, J. Fire Sci. 14 (1996) 426-442.
[9] E.N. Peters, J. Applied Polymer Sci. 24 (1979) 1457-1464.
[10] B. Schartel, Materials 3 (2010) 4710-4745.
[11] S.V. Levchik, and E.D. Weil, J. Fire Sci. 24 (2006) 345-364.
[12] C.P. Fenimore, and G.W. Jones, Combust. Flame 10 (1966) 295-301.
[13] G.T. Linteris, Flame Suppression Chemistry, In: Advanced Technology for Fire Suppression in Aircraft, The Final Report of the Next Generation Fire Suppression Technology Program, NIST SP 1069, 2007, p. 119.
[14] J.A. Kaizerman, and R.E. Tapscott, Advanced Streaming Agent Development, Volume II: Phosphorus Compounds, NMERI 96/5/32540, New Mexico Engineering Research Institute, Albuquerque, NM, 1996.
[15] J.L. Lifke, T.A. Moore, and R.E. Tapscott, Advanced Streaming Agent Development, Volume V: Laboratory-Scale Streaming Tests, NMERI 96/2/32540, NMERI, Albuquerque, NM, 1996.
[16] M.A. McDonald, T.M. Jayaweera, E.M. Fisher, F.C. Gouldin, Combust. Flame 116 (1999) 166-176.
[17] N. Bouvet, G.T. Linteris, V.I. Babushok, F. Takahashi, V.R. Kattta, R.H. Krämer, Fire and Materials, submitted, 2015.
[18] G.T. Linteris, V.R. Kattta, F. Takahashi, Combust. Flame 138 (1-2) (2004) 78-96.
[19] F. Takahashi, G.T. Linteris, V.R. Kattta, Proc. Combust. Inst. 31 (2007) 2721-2729.
[20] F. Takahashi, V.R. Kattta, G.T. Linteris, V.I. Babushok, V.I., Proc. Combust. Inst. 35 (2014).
[21] F. Takahashi, V.R. Kattta, G.T. Linteris, V.I. Babushok, V.I., Fire and Materials, San Francisco, 2015.
[22] V.R. Kattta, L.P. Goss, W.M. Roquemore, AIAA J. 32 (1994) 84.
[23] W.M. Roquemore, V.R. Kattta, J. Visualization 2 3/4 (2000) 257-272.
[24] M. Frenklach, H. Wang, M. Goldenberg, G.P. Smith, D.M. Golden, C.T. Bowman, R.K. Hanson, W.C. Gardiner, V. Lissianski, GRI-Mech—An Optimized Detailed Chemical Reaction Mechanism for Methane Combustion, Report No. GRI-95/0058, Gas Research Institute, Chicago, IL, 1995.
[25] O.P. Korobeinichev, V.M. Shvartsberg, A.G. Shmakov, T.A. Bolshova, T.M. Jayaweera, C.F. Melius, W.J. Pitz, C.K. Westbrook, Proc. Combust. Inst. 30 (2004) 2350-2357.